Isolating the role of mesoscale eddies in mixing of a passive tracer in an eddy resolving model

James Booth[1] and Igor Kamenkovich[2]

Received 18 August 2007; revised 2 December 2007; accepted 11 February 2008; published 16 May 2008.

[1] This study examines the role of mesoscale eddies in distribution of chlorofluorocarbon (CFC) in a numerical model of the North Atlantic. Our main conclusions are based on a comparison of two eddy-resolving experiments, one with and one without eddy advection of CFC. The CFC distributions in these two experiments exhibit substantial differences within the subpolar gyre. In particular, in the presence of eddies the horizontal distribution of CFC in the upper 1000 m is more uniform and the CFC concentration is lower in the lower 1500 m. Our analysis demonstrates that these basin-wide differences are caused by the interactions of eddy advection with convection and mean advection in several isolated locations. The corresponding eddy flux divergence terms are spatially non-uniform in magnitude; their effects are often nonlocal and sometimes work against the spreading of CFC being carried out by the mean advection. These conclusions are further confirmed by a third experiment, in which the eddy advection was replaced by a down-gradient diffusive parameterization. Our results demonstrate that advection by mesoscale eddies is crucial to the mixing of atmospheric gasses into the ocean, and outline difficulties in representing eddies by the down-gradient diffusion.

Citation: Booth, J., and I. Kamenkovich (2008), Isolating the role of mesoscale eddies in mixing of a passive tracer in an eddy resolving model, *J. Geophys. Res.*, *113*, C05021, doi:10.1029/2007JC004510.

1. Introduction

[2] Understanding the role of mesoscale eddies in ocean circulation represents a long-standing problem in physical oceanography. It has been recognized that eddies are not simply products of baroclinic instability of the mean flow, but rather play an active role in setting ocean stratification and circulation; see, for example a review by *McWilliams* [2008]. Understanding eddy behavior will not only expand our understanding of ocean dynamics, but will assist in modeling ocean circulation on scales from basin-wide to mesoscale. Progress in studies on mesoscale eddies, however, is complicated by severe lack of observational data and challenges in simulating eddies in comprehensive climate models.

[3] Several studies have explored the effects of eddies on the midlatitude ocean stratification in idealized numerical simulations. Mesoscale eddies have been shown to result in significant cross-isopycnal mixing within the surface mixed layer, but to act predominantly along isopycnal surfaces beneath it. The near-surface diapycnal fluxes act to balance the Ekman pumping within a subtropical gyre and play a central role in the potential vorticity budget [*Radko and Marshall*, 2004]. The along-isopycnal eddy fluxes of buoyancy act to flatten isopycnal surfaces, counteracting overturning effects of surface buoyancy fluxes and winds [*Karsten et al.*, 2002; *Marshall et al.*, 2002; *Marshall and Radko*, 2003]. Eddy fluxes help to sustain the main thermocline by partially balancing upwelling [*Henning and Vallis*, 2004], and, in the absence of upwelling, vertical diffusion [*Cessi and Fantini*, 2004].

[4] The mesoscale is not routinely resolved by modern climate models, and the effects of eddies are instead parameterized, or expressed in terms of large-scale properties. These parameterizations are predominantly based on the assumption of down-gradient diffusive mixing of properties with the diffusion coefficients determined empirically and often taken to be constants. Several studies, however, cast doubt on the ability of such schemes to accurately represent effects of eddies. Analysis of eddy-resolving simulations suggests strongly non-uniform distribution of diffusion coefficients and even presents evidence for the existence of up-gradient fluxes of temperature and salinity [*Gille and Davis*, 1999; *Nakamura and Chao*, 2000; *Roberts and Marshall*, 2000]. Eddy fluxes of tracers are, in fact, expected to be directed down-gradient only if there is a downstream increase in tracer variance or there is a strong dissipation of tracer variance [*Wilson and Williams*, 2006]. The importance of such non-uniformity in the diffusion coefficient and significance of the up-gradient tracer fluxes have never been estimated.

[5] Analysis of the effects of eddies on stratification and circulation represents a challenging problem. The large-

[1]Department of Atmospheric Sciences, University of Washington, Seattle, Washington, USA.
[2]Rosenstiel School of Marine and Atmospheric Science, University of Miami, Miami, Florida, USA.

Copyright 2008 by the American Geophysical Union.
0148-0227/08/2007JC004510

scale, non-eddying fields are determined by several processes, such as the large-scale advection in zonal, meridional and vertical directions, advection by eddies, mixing and convection. In theory, the most straightforward and accurate way to determine the importance of a particular dynamical term is to remove it from the system and analyze the resulting changes. In particular, in order to isolate the role of eddy fluxes, one has to consider an ocean *without eddies* and contrast it to the complete system. In practice, this approach is not always plausible, because any high-resolution simulation will generate mesoscale variability. One common approach to "filter out" eddies is to contrast eddy-resolving and non-eddy-resolving simulations. Eddy parameterization in the latter models, intended to substitute for unresolved eddies, can also be evaluated. However, time-mean circulation is so different between these simulations, with some differences possibly caused by the change in resolution, that understanding of the role of eddies becomes very difficult to achieve. In other words, such analyses cannot separate direct effects of eddies from effects of increased horizontal resolution on the mean, non-eddying fields.

[6] Our approach to the problem is to consider the distribution of a dynamically passive tracer in an off-line model. As will be shown in this manuscript, use of an off-line model with prescribed circulation simplifies separation of eddy effects on a passive tracer from those of the mean currents. For the analysis, we choose chlorofluorocarbon (CFC), whose industrial release began approximately 70 years ago. Analysis of the distribution of this tracer represents a convenient tool for studies of the ocean circulation and water mass formation, and for assessing ocean models [*England and Maier-Reimer*, 2001]. Such analysis will also help in understanding the role of eddies in mixing atmospheric gasses, including carbon dioxide, into the ocean.

[7] CFC simulation in ocean models is highly sensitive to horizontal resolution and parameterization of subgrid mixing in GCMs [*Beismann and Redler*, 2003; *Gupta and England*, 2004]. In particular, *Beismann and Redler* [2003] and *Gupta and England* [2004] demonstrate that high resolution is required for more accurate representation of the CFC transport in the deep western boundary current, and of sharpness of CFC fronts. However, separation of the effects of eddy CFC transports from the effects of the more accurate simulation of the steady currents is not straightforward in these studies. The present study is the first to explicitly isolate the effects of mesoscale eddies and their transport on CFC distribution.

[8] The paper is organized as follows. The tools and methods of this study are described in section 2. The eddy-resolving numerical model of the North Atlantic and the simulated ocean state is described in sections 2.1 and 2.2, followed by the description of the off-line model for the CFC distribution. The main results of the analysis of the role of eddies in CFC distribution are presented in section 3. We begin by contrasting our eddy-resolving simulation with its non-eddy-resolving equivalent in section 3.1. As will be shown in this section, the analysis is complicated by large differences in the mean circulation and stratification. We then proceed in section 3.2 with the analysis of the off-line eddy-resolving simulations with eddy advection removed and discuss effects of such removal on CFC distribution. In section 4, we draw some conclusions on the role of eddies in distribution of CFC, and on challenges of parameterizing these effects in climate models.

2. Model Description and Experimental Design

2.1. Numerical Model

[9] A study of the complex role of mesoscale eddies calls for a model that preserves a sufficient degree of realism in order to ensure adequate simulations of the gross features of the oceanic state. At the same time, it is desirable to work with a model that is computationally efficient, and has a number of idealized features that simplify interpretation of the results. The simulations described in this study are carried in such "intermediate complexity" model. The computer model used is the Modular Ocean Model, (MOM, hereafter) version 3.0 [*Pacanowski and Griffies*, 1999], which solves the primitive equations on depth levels. The domain for the model is most of the northern hemisphere Atlantic Ocean. The latitudinal range is 15°N to 60°N. This spans from Cuba to just below the southern tip of Greenland. It includes the two wind-driven gyres, but excludes the northern half of the Labrador Sea and the GIN (Greenland, Iceland and Norwegian) Seas. The implications of the limited domain and other idealizations in the model for circulation and CFC distribution are discussed in sections 2.2 and 2.4. The longitudinal range is 80°W to 10°W, spanning the entire Atlantic. Unlike most idealized double-gyre studies that use rectangular domains, this model has a realistic domain to improve the representation of the Gulf Stream. The velocities use no-slip boundary conditions at the sidewalls, the north and south walls and at the bottom. The bathymetry includes sea-shelves; however the model depth is fixed at 3000 m. In the Atlantic Ocean, 3000 m is the approximate depth at which the North Atlantic Deep Water (NADW) sits atop of the Antarctic Bottom Water [*Schmitz*, 1996] The restricted depth of the domain allows the experiment to avoid difficulties of simulating low-latitude circulation of the bottom water in a single-hemisphere model and reduces the spin-up time, since the deepest layers take the longest to equilibrate. The topography is partially distorted, which has some effects on the barotropic circulation. However, more than 50 per cent of the subpolar gyre, our main region of interest, is shallower than 3000 m.

[10] The horizontal grid-size permits resolution of mesoscale eddies; grid spacing is uniform at 1/8 degree in both latitudinal and longitudinal directions. There are ten depth levels, which are close together at the surface and farther apart at depth; the depths of the temperature and salinity points are: 25 m, 87 m, 185 m, 338 m, 560 m, 861 m, 1238 m, 1685 m, 2187 m, and 2725 m. This choice of vertical levels was made to optimize the trade-off between speed of computation and resolution of stratification. The model does not have a mixed layer parameterization. Vertical diffusion is kept to a value suggested by observations in the ocean above rough topography, 10^{-5} m^2 s^{-1} [*Ledwell et al.*, 1993; *Toole et al.*, 1994]; the diffusion is semi-implicit. Horizontal viscosity is 200 m^2 s^{-1}. With the zonal grid spacing of 12 km (at 30°N), the Munk layer (20 km) is minimally resolved; smaller viscosity will affect the simulation of the Gulf Stream [*Smith et al.*, 2000]. Higher viscosity would further suppress the already weaker

Table 1. Characteristics of the Model Experiments

	FULL_ADV	MEAN_ADV	MEAN_PLUS	NER
Resolution	1/8° × 1/8°	1/8° × 1/8°	1/8° × 1/8°	1° × 1°
Topography	1° × 1°	1° × 1°	1° × 1°	1° × 1°
Convection	implicit	implicit	implicit	implicit + explicit
Mesoscale eddies	resolved	removed	parameterized	parameterized
Horizontal viscosity ($m^2 s^{-1}$)	200	200	200	10^4
Vertical viscosity ($m^2 s^{-1}$)	10^{-3}	10^{-3}	10^{-3}	10^{-3}
Horizontal diffusion ($m^2 s^{-1}$)	10	10	10	0
Vertical diffusion ($m^2 s^{-1}$)	10^{-5}	10^{-5}	10^{-5}	10^{-5}
Isopycnal mixing ($m^2 s^{-1}$)	0	0	100	500
Thickness diffusivity ($m^2 s^{-1}$)	0	0	0	500

than observed eddy kinetic energy. The horizontal diffusion is 10 $m^2 s^{-1}$. Convection in the model is modeled by the so-called implicit scheme [*Pacanowski and Griffies*, 1999]: If there is an unstable layer the vertical diffusion is set to a very large value to allow homogenization of the column of instability. A second order advection scheme is used.

[11] Annual-mean meridional and zonal components of the wind stress are derived from the NCEP 1979–2001 reanalysis. The exclusion of the seasonal cycle simplifies analysis of the eddy effects on a transient tracer (CFC). The surface boundary conditions are restoring to annual-mean climatological values of sea-surface temperature and salinity, both derived from the high resolution (1/4 degree) analyses of the World's Oceans, version 2 [*Boyer et al.*, 2005]. The restoring timescales are 60 and 180 days for temperature and salinity (for a 50 m top layer). Such highly idealized surface conditions were chosen for their simplicity and ability to maintain realistic surface distribution of density. The restoring conditions at the surface will shorten the life-time of surface buoyancy anomalies; the restoring timescale (60 days for temperature) is, however, long enough to allow mesoscale variability on the timescale of several weeks. At the southern and northern lateral boundaries there are also restoring boundary conditions to simulate buoyancy exchanges. Levitus temperature and salinity data for 15°N and 60°N are used with a 180-day restoring timescale. These lateral "sponge boundaries" help to maintain realistic stratification in the model; see below. Note that these restoring surface and lateral boundary conditions do not impose any variability on the simulated ocean; all eddy variability is therefore purely intrinsic.

[12] To address the effects of increased resolution, we will also compare our standard eddy-resolving (ER) simulations to the non-eddy-resolving (NER) simulations in a coarse-resolution model. A one degree by one degree, NER model with the same vertical resolution, computational domain and boundary conditions as the ER model is spun-up to a steady state and run for 70 years with the CFC flux described by equation (1). This model parameterizes the sub-grid scale motions (SGS) using the Gent-McWilliams scheme (GM; *Gent and McWilliams* [1990]); see Table 1 for details.

2.2. Simulated Ocean State

[13] To accelerate the convergence to a steady state, we initialized our eddy-resolving model with a quasi-steady state obtained in a similar model at 0.25 degree resolution. Similarly, 0.5 degree and 1 degree models were used to initialize the 0.25 degree model state in a series of runs with increasing horizontal resolution. The cumulative integration time is 4100 years; at its highest resolution, the model integrated for 25 years. In the resulting near-steady state, the drift for the model's domain-averaged temperature is less than 0.3°C over 100 years. For comparison, the mesoscale variability in temperature is much stronger with the area-averaged amplitude (standard deviation) varying from 0.7°C at the surface to 0.1°C near the bottom and a timescale of less than a month.

[14] The wind-forcing leads to a double-gyre circulation. The maximum transport of the modeled Gulf Stream is 81 Sverdrups (Sv), and this occurs at 35° N, near 72°W. At this location observational estimates for the transport are 85 Sv [*Schmitz*, 1996]. The model's Gulf Stream correctly separates from the western boundary and flows eastward near 35°N. The path of the current after it leaves the coast is, however, unsteady and the meanders are large. As a result, the time-mean surface velocities exhibit a Gulf Stream extension that is too broad and weak. In addition, part of the model's Gulf Stream quickly turns north again and does not turn east until it reaches 40°N and 45°W. These problems are typical of many ocean models, even those at very high resolution, [e.g., *Nakamura and Chao*, 2000]. The southward flowing portion of the subpolar gyre is the western boundary current referred to as the Labrador Current. Near 47°N, this current separates from the coastline, feeding into the Gulf Stream extension, the model's analog of the North Atlantic Current. This component of the North Atlantic Current, originating from the Labrador Current and characterized by high concentrations of CFC, will be called the *subpolar gyre return flow* (SRF hereafter, shown in Figure 1 by the current vectors near 57°N by 48°W).

[15] On a basin average, the stratification in the model resembles observations reasonably well. The model agrees closely with Levitus [*Boyer et al.*, 2005] observational data for 50°N and 40°N, where the model's isopycnals have a gradual meridional tilt. The model has waters which are less dense than those observed in nature north of 55°N, at 40°W. This bias is caused by the model boundary at 60° N, which forces the less dense waters advected by the Gulf Stream extension to circulate toward the west more than they do in nature. In the subtropical gyre, the model qualitatively captures the density distribution across the entire latitudinal domain. The lateral sponge boundaries greatly help to make the simulated stratification more realistic, as the comparison with model runs without the lateral sponge boundaries reveals (not shown here). The sponges cannot, however, fully substitute for the lack of the Southern Hemisphere in

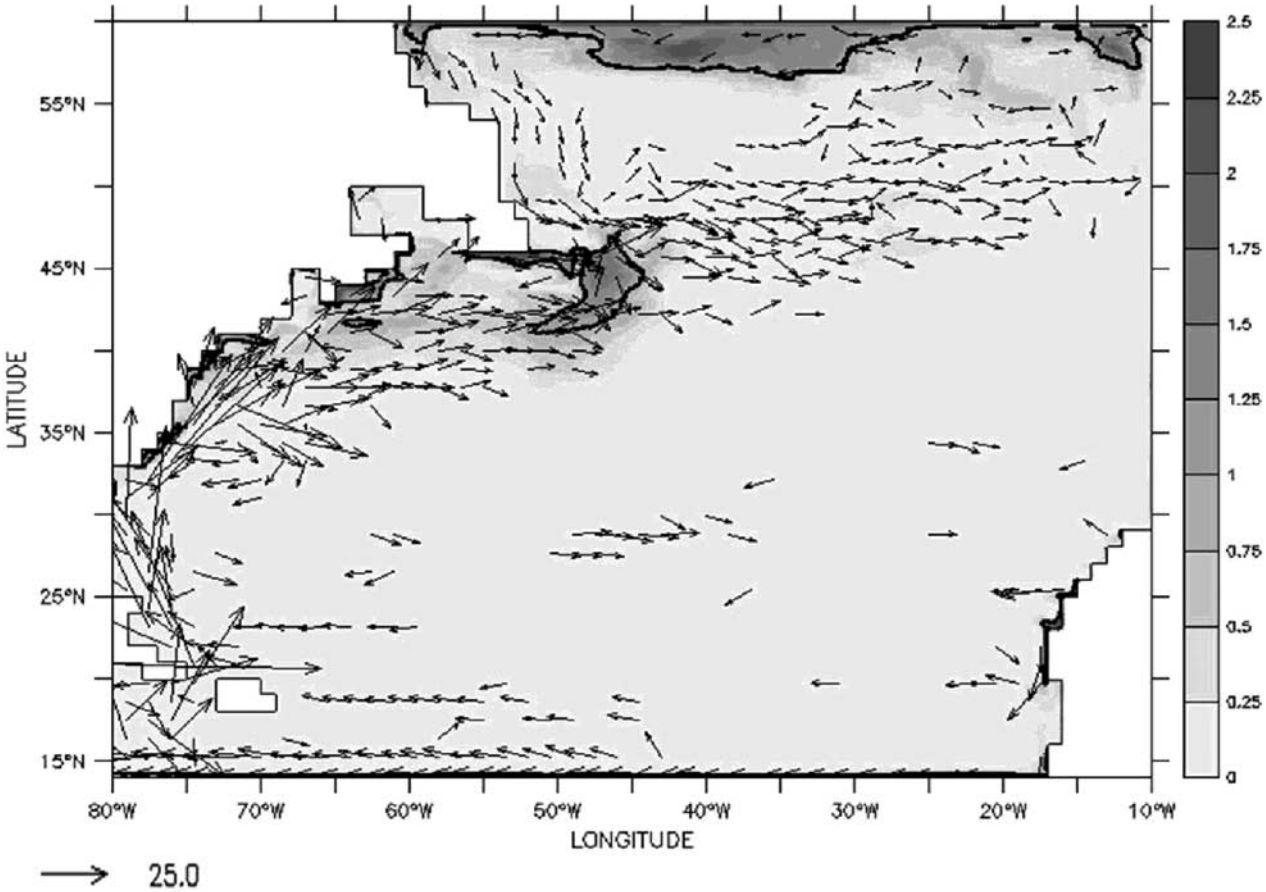

Figure 1. Surface flux of CFC, averaged over years 41 to 70. Units: $\times 10^{-3}$ pmol kg^{-1}s^{-1}. Solid contour line has a value of 1. Overlayed are the time-averaged velocities in the first layer of the model, scale is shown in the bottom right with units of cms^{-1}. Vectors less than 5 cms^{-1} are omitted.

the model, which leads to remaining biases in the model stratification. Most notably, the simulated pycnocline is somewhat sharper and 50–75 m shallower than in the observations. Moreover, in order to simulate lateral heat and salt exchanges, the restoring conditions require systematic biases in the temperature and salinity at the southern and northern lateral boundaries of the domain. In particular, sponge boundaries can simulate northward heat flux into the domain only if the ocean at the southern boundary is systematically colder than the observed, which leads to moderate but artificial shoaling of isopycnals. Several idealizations in the model, including coarse vertical resolution, the absence of parameterization for the boundary layer mixing and the lack of seasonal cycle also result in too shallow a mixed layer.

[16] Consistent with a shallow pycnocline [e.g., *Gnanadesikan*, 1999], the meridional overturning circulation (MOC) is too weak and shallow in the model, and amounts to 10Sv at its maximum. The limited model domain is the main reason for the weak overturning. Most importantly, the lack of a dynamical southern boundary removes northward volume flux into the domain that helps to drive the overturning circulation [*Gnanadesikan*, 1999]. The implications of the distorted geometry of the Labrador Sea for MOC are less clear, since a recent study by *Pickart and Spall* [2007] suggests a moderate role of the Labrador Sea in the Atlantic MOC. The vertical diffusivity coefficient is set to a value suggested by observations and is several times smaller than values typically used in single-hemisphere ocean models. Increasing diffusivity to artificially high values helps to enhance the overturning and deepen the pycnocline [*Bryan*, 1987]. The enhanced MOC in this case is, however, due to unrealistically strong diapycnal mixing and upwelling at mid- and low latitudes. By choosing the low value of vertical diffusivity, we limit the amount of diapycnal mixing to more realistic levels.

[17] The deep western boundary current begins in the north-west corner of the model, as part of the subpolar gyre's circulation. It moves east along the deep portion of the SRF to an area near 55° N by 30°W. At that point it turns to the south and west and travels back to the western boundary. The current hugs the western boundary of the model south of 40°N. From observational studies of CFC, this is the region in which a strong coast-hugging deep western boundary current is located [*Dutay et al.*, 2001].

[18] Most of the differences between the simulated circulation and stratification in the eddy resolving (ER) and NER simulations are consistent with those reported in other studies [*Solovev*, 1999; *Nakamura and Chao*, 2000; *Henning and Vallis*, 2004]. The time-mean circulation is drastically

different between the ER and NER simulations. Because of coarse resolution and high horizontal viscosity, the Gulf Stream in the NER model is weaker and less concentrated, and does not separate from the coastline in a concentrated flow. Instead, at 48°N, it fans out to the north, northeast and east. Unlike the ER model which simulates the slopes of the outcropping isopycnals more realistically, the NER model exhibits isopycnals that are too vertical near the surface in the subpolar gyre. Also, the main pycnocline is shallower in the NER model than in the ER model. These differences are partly due to the replacement of the SGS parameterizations in the NER model with resolved eddy advection in the ER model. In particular, *Henning and Vallis* [2004] report that the adiabatic eddy advection supports the main pycnocline in their ER model, by supplying cold water from high latitudes. Parameterized GM advection may overestimate the strength of this effect leading to too shallow a pycnocline in NER model.

2.3. Offline Model

[19] As discussed in the Introduction, identification of the role of eddies in the distribution of momentum and density is challenging, due to complex dynamical coupling between eddies, mean circulation and stratification. In this study, we choose to analyze the effects of eddies on a dynamically passive tracer. For its simulation, we designed an offline model, which advects all tracers with velocities calculated by a full, "online" model discussed in the previous section; see also discussion of the off-line simulations by *Gupta and England* [2004] and *Bey et al.* [2001]. Running the model "offline" means that the velocities are prescribed (read-in), not calculated, but the model is otherwise identical to the online version. Eight years of velocities were saved from the spun-up online run, and these eight years are used on a loop to create a 70-year offline model run. The temperature and salinity in the offline model are solved for as if it was an online model. As will be shown below, the temperature and salinity in the offline run stay very close to their values in the online circulation, so the density and velocity distribution remain mutually consistent. The calculation of temperature and salinity on every time step allows the offline model to have convection that is very similar to that in the online model.

[20] We run the offline model with the time step of 1 hour. Cubic interpolation of 5 day velocity data is used to calculate tracer advection velocities at every time step. To make sure that this exclusion of high variability velocities does not introduce significant biases in temperature and salinity, we compared online- and offline-calculated T and S fields. After 70 years, the offline fields are never more than 3% different from the online fields at any location. Further, for 95% of the model, the offline T and S fields are never more than 1% different from the online case. Running the model with daily velocities led to a bias with a similar magnitude.

[21] To test that the biases in the offline model do not influence the passive tracer distribution, our NER model was run online and offline with CFC. After a 70 year run, both the CFC and T/S difference in the online and offline model was less than 1% at all locations. These results suggest that the CFC field will not be significantly biased by the offline calculation in the ER model, and that the relative biases in temperature, salinity and CFC will be equally small. Since the CFC surface flux depends on the temperature and salinity, which are restored at the surface, this strong agreement can be expected.

[22] These remaining very small model biases are easily offset by the advantages of the offline model. The first advantage is a faster run-time. The online model takes 5.5 days to run one model year on a single 667 MHz processor, while the offline model only takes 20 h. The second advantage is that the offline model can be run using different prescribed velocity fields. This allows us to perform the experiment discussed in this study. Specifically, we perform a model integration in which the full velocities advect the T and S fields, but only the time-averaged velocity advects passive tracer. This is discussed in greater detail in section 3.2.

2.4. CFC Surface Flux and Distribution

[23] The passive tracer added to the model is chloroflourocarbon-11 (hereafter, CFC-11 or CFC). CFCs are inert in the ocean, and so they are conserved. Since the start of their industrial output in 1930, the atmospheric concentration for CFC-11 has been well monitored. The global atmospheric concentration of CFCs was growing for the period 1930 to 2000; see, for example, *England et al.* [1994].

[24] *England et al.* [1994] compared observed fluxes with those obtained using various parameterizations of the flux in an ocean model. The study found that the most realistic parameterization of the surface flux $F_{surface}$ is accomplished with the following equation:

$$F_{surface} = k(\alpha C_A - C_O) \tag{1}$$

[25] In equation (1), the piston velocity, k is determined using the formula of *Wanninkhof* [1992], as a function of wind speed (wind speeds are derived from the NCEP 1979–2001 reanalysis), the Schmidt number for CFC, and an empirical constant. The variable α is the gas solubility coefficient, which is a function of the SST and surface salinity. The function for α was derived empirically from laboratory studies by *Warner and Weiss* [1985]. High winds and cold temperatures increase the solubility of the gas in water, creating a larger flux. The atmospheric concentration is C_A and the oceanic concentration is C_O. The flux in this study differs from that of *England et al.* [1994] in that it is required to be greater than or equal to zero. That is to say, the parameterization does not allow for out-gassing. Since CFC-11 concentrations increase yearly, and the model uses yearly rather than seasonal heat and salinity fluxes, this specification is reasonable. To verify this, the NER model was ran with CFC for outgassing on and off. The results were only different in the southern portion of the subtropical gyre. The specification of no outgassing in the eddy-resolving model allowed the offline model to be run at a larger time step.

[26] For the last 40 years of the model run, the CFC surface flux (Figure 1) is nearly in steady state, with the bulk of the CFC entering the ocean north of 45°N. To the zeroth order, the sea surface temperature is most important for determining the CFC flux, causing the fluxes to be much larger in the high latitudes, as compared to the mid- and low latitudes. However, within the high latitudes the flux max-

imum does not coincide with the areas of coldest SST. Instead, the maxima are in regions of active convection and regions of strong ocean currents. Active convection along the northern boundary continuously depletes the surface CFC, leading to a large CFC uptake. The strong advection of warm, low-CFC surface waters from the south by the Gulf Stream is also an ideal preconditioning for a large CFC surface flux. Cooling of these waters further enhances the CFC uptake.

[27] The CFC concentrations on three density levels are shown in Figure 2. The levels are chosen to represent the upper-, mid- and deep-depths, with the potential density (referenced to the surface) anomalies σ_θ equal to 26.6, 27.7, and 27.9. In the subtropical gyre, CFC is drawn into the upper layers, however it does not penetrate any farther downward. The majority of the CFC spreads throughout the subpolar gyre interior in the upper- and middepths, and then moves into the deep water in the northernmost regions of the model. On $\sigma_\theta = 27.7$ in Figure 2, the circulations of the Labrador Current and the SRF are highlighted by high CFC concentrations. These are locations of strong mean advection, which move the CFC drawn downward by convection around the edges of the subpolar gyre. There is also significant penetration of CFC into the middle of the subpolar gyre. From the subpolar gyre, some of the CFC is advected into the northeastern part of the subtropical gyre.

[28] The CFC distribution in the model is generally consistent with observations. In particular, the near uniform spreading of CFC throughout the eastern subpolar gyre interior is in qualitative agreement with observational data [*Dutay et al.*, 2001]. The CFC distribution at middepth also does not exhibit an unrealistic local minimum that is characteristic for non-eddy-resolving simulations; see *Beismann and Redler* [2003] and Figures 3a and 3c. However, the amount of CFC drawn into the model is less than that observed in nature, and there is less CFC in the model's deep waters. The weakness of the model's MOC is the most likely reason for the underestimated CFC uptake. A stronger MOC would advect more of the CFC drawn into the subpolar gyre southward. The surface fluxes would then increase in response to this removal of CFC from the subpolar gyre. The distorted geometry of the Labrador Sea and the lack of GIN seas can also be a factor causing biases in the CFC distribution. *Beismann and Redler* [2003] and *Gupta and England* [2004] both attribute a significant amount of CFC uptake to the these regions. Nevertheless, less than 7 per cent of the observed CFC in the North Atlantic (north of 14°N) end up stored north of 60°N (Glodap data set [*Key et al.*, 2004]). The lack of a seasonal cycle coupled with the absence of a mixed layer parameterization also contribute to the biases of the CFC uptake in the model, as both factors have been shown to affect CFC simulation [*England et al.*, 1994; *Gupta and England*, 2004].

[29] The CFC distributions in the ER and NER simulations differ throughout the entire subpolar gyre, consistent with previous studies. Significantly more CFC reaches the deep water in the NER run compared to the ER simulation; see the cross-section at 40° W (Figures 3a and 3c). *Beismann and Redler* [2003] similarly noted a decrease in CFC concentration in the deep waters of their subpolar gyre when they increased resolution from 4/3° to 1/3°. The deep-depth CFC maximum at 45°N associated with DWBC advection is deeper in NER simulation. In contrast, the CFC concentrations at approximately 500 m in the subpolar gyre interior of the NER simulation are very small. This CFC minimum at the middepths is a bias that has been observed in other NER modeling studies of CFC, [*Beismann and Redler*, 2003; *Dutay et al.*, 2001, Figure 1]. This bias is not observed in the ER simulation, which brings the results closer to observations at the middepths. Beismann and Redler's study of increasing the horizontal resolution also shows an increase in modeled CFC content in the upper subpolar gyre, especially along the boundary currents, which we also find.

[30] These differences in CFC distributions between the ER and NER models can, in large part, be explained by the differences in the time-mean circulations. In particular, a deeper pycnocline and MOC cell in NER, as compared to the ER simulations, results in a deeper CFC maximum in NER model. The differences in CFC concentrations within the subpolar gyre are also partly due to the differences in the Gulf Stream circulation. The Gulf Stream in the NER simulation does not fully separate from the coast, resulting in northward currents in the center of the western portion of the subpolar gyre. These currents distort the cyclonic flow of the subpolar gyre forcing the SRF northeastward which advects the CFC away from the gyre interior and into the sinking regions of the model. Thus the deep water in the NER model has an additional source of CFC, while the interior of the gyre has an additional sink.

3. Role of Eddies in Distribution of CFC

[31] To isolate the effects of eddies on CFC distribution, we have carried out an eddy resolving off-line experiment in which the passive tracer is advected by the time-mean flow without eddies. In this experiment (called "MEAN_ADV"), the temperature and salinity are advected by the full velocities. This allows the MEAN_ADV run and the original offline ER run (hereafter "FULL_ADV") to have the exact same density distribution and convection. The only difference between MEAN_ADV and FULL_ADV is the velocities used for advecting the CFC. This is arguably the most accurate and straightforward way to isolate eddy effects on a dynamically passive tracer.

[32] The common assumption that eddies act to homogenize tracers on isopycnal surfaces motivated the design of a third model experiment MEAN_PLUS, in which we add isopycnal diffusion to MEAN_ADV. For simplicity of the analysis of the sensitivity of the CFC distribution to the intensity of downgradient mixing, we choose the simplest parameterization scheme, the isopycnal diffusion with a constant coefficient. The simulations were carried out with the diffusion coefficient equal to 10 $m^2\ s^{-1}$, 50 $m^2\ s^{-1}$, 100 $m^2\ s^{-1}$, and 1000 $m^2\ s^{-1}$. In the remainder of the article, we present results for 100 $m^2\ s^{-1}$; the value is five to ten times lower than the one typically used in coarse-resolution studies. As will be shown, the 100 $m^2\ s^{-1}$ value resulted in too much uptake of CFC at middepth; the larger values lead to even larger deviations from FULL_ADV, while the smaller values result in biases very similar to MEAN_ADV.

[33] For the MEAN_ADV and MEAN_PLUS model runs, the velocity field used is an eight-year time average.

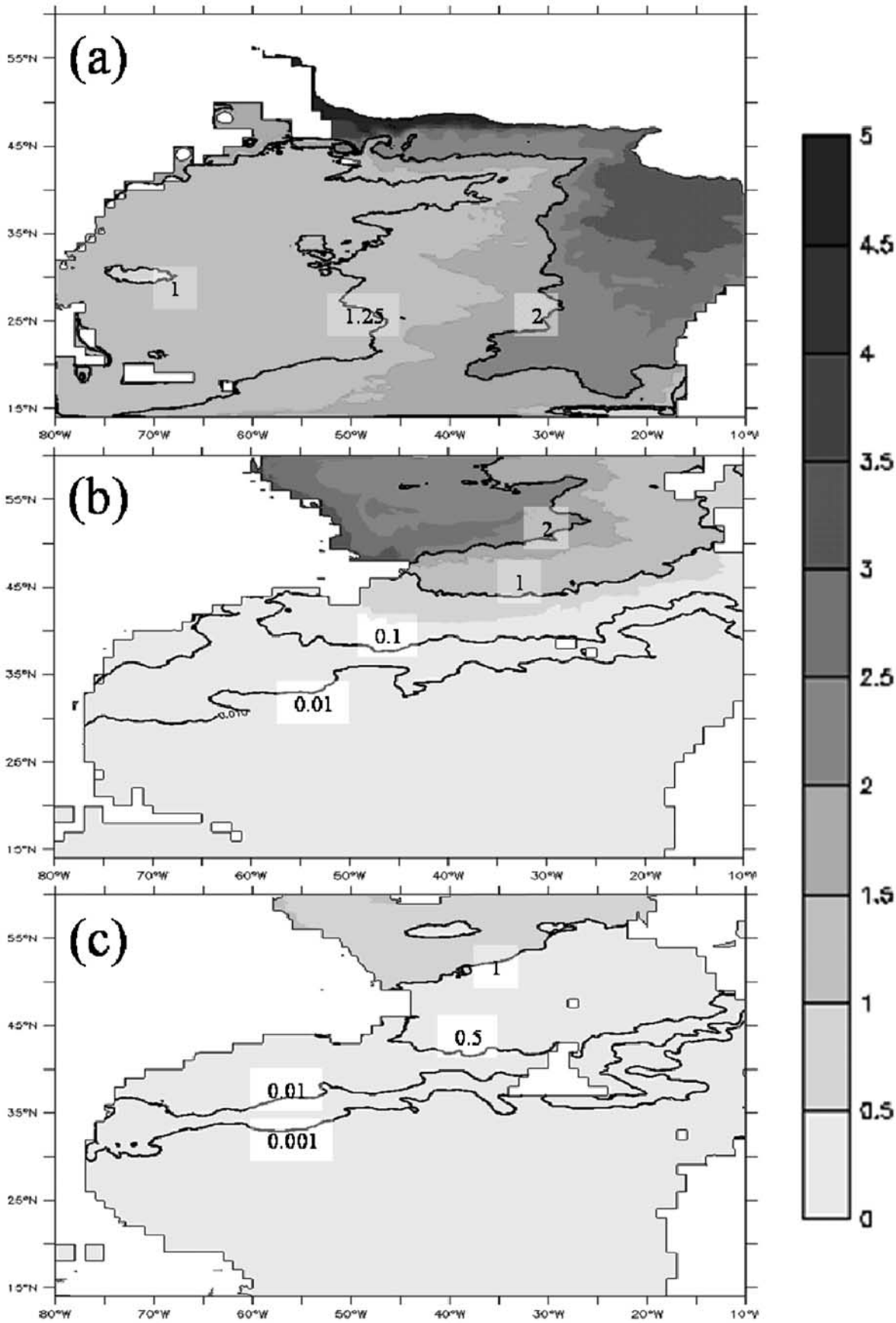

Figure 2. CFC concentration at year 70 for three isopycnal levels of FULL_ADV, numbers on the figure are values for the dark contour lines: (a) $\sigma_\theta = 26.6$, (b) $\sigma_\theta = 27.7$ and (c) $\sigma_\theta = 27.9$. Units: pmol kg^{-1}.

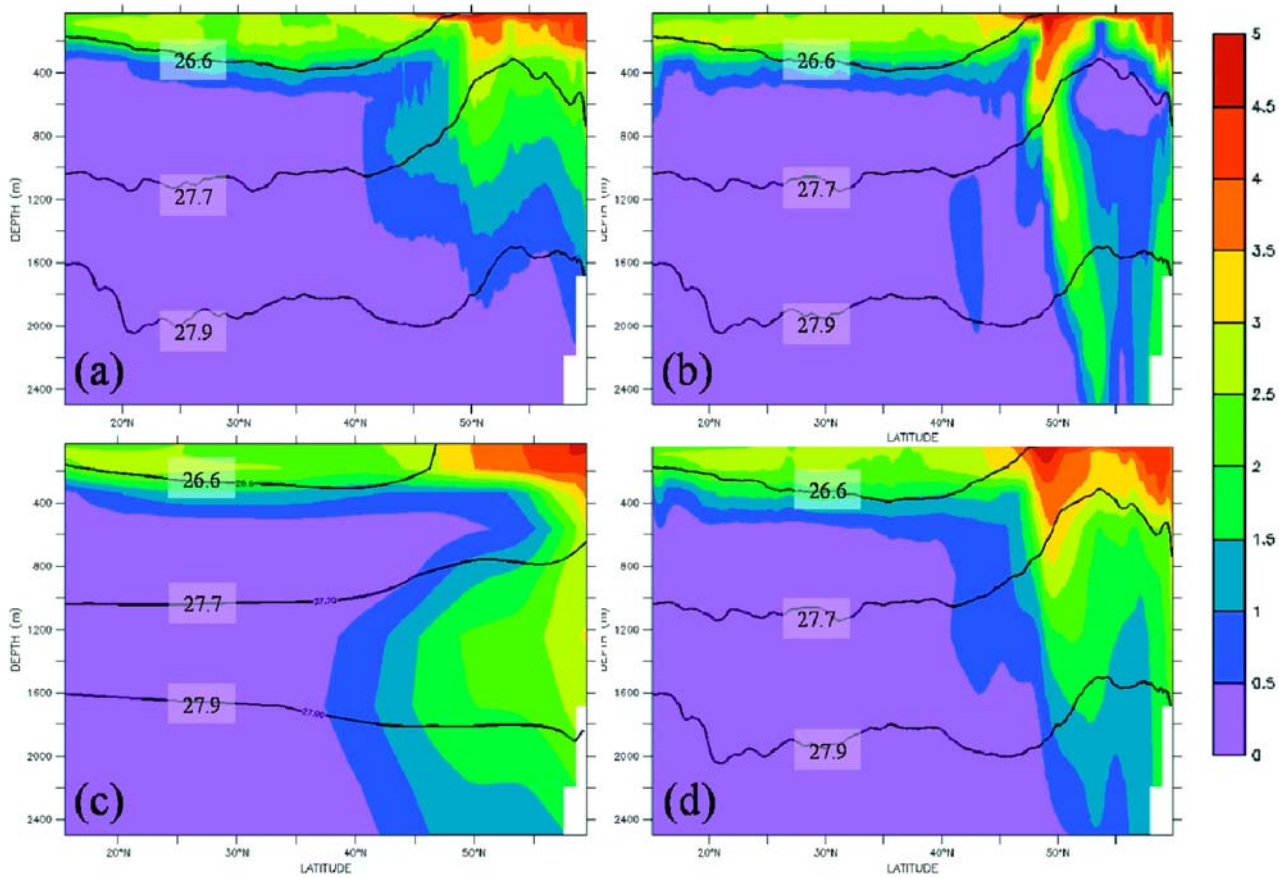

Figure 3. Cross-section at 40°W showing CFC concentration at year 70. (a) FULL_ADV, (b) MEAN_ADV, (c) NER and (d) MEAN_PLUS. Units: pmol kg^{-1}. Overlayed are the contour lines showing the isopycnal levels plotted in Figures 2, 4 and 5.

Since mesoscale variability occurs on timescales of weeks to months, an eight-year time-average of the velocity can be assumed to have the mesoscale variability averaged out. This time-averaging will also remove part of the interannual variability in the model. Thus the differences between FULL_ADV and MEAN_ADV can potentially represent differences due to variability on timescales longer than the mesoscale. A comparison of two-year and eight-year mean states (not shown), suggests that the interannual variability is small. It is also noteworthy that, since the eddies partially determine the mean state of the ER model, they have an indirect effect on the CFC distribution in MEAN_ADV and MEAN_PLUS – through the mean state. Thus MEAN_ADV and MEAN_PLUS cannot be thought of as the same thing as a run without eddies [*Ladd and Thompson*, 1998]. However, time averaging removes the *direct* effects of eddy advection on the distribution of CFC, and these effects are the focus of this study.

[34] To aid in clarifying the role of the eddies in our analysis, we separate velocities u and CFC concentration C into the time-mean ($\bar{\mathbf{u}}$, $\bar{C}$) and eddy terms (u′, C'). After averaging in time, the CFC fluxes split into two terms, mean and eddy:

$$\overline{\mathbf{u}C} = \bar{\mathbf{u}} \cdot \bar{C} + \overline{\mathbf{u}'C'} \tag{2}$$

[35] The tracer conservation equation in FULL_ADV then transfers to:

$$\frac{\overline{\partial C}}{\partial t} + \nabla \cdot (\bar{\mathbf{u}} \cdot \bar{C}) + \nabla \cdot \left(\overline{\mathbf{u}'C'}\right) = k_h\left(\bar{C}_{xx} + \bar{C}_{yy}\right) + k_v(\bar{C}_{zz}) \tag{3}$$

[36] In this equation, the first term is the time-tendency of the CFC. The second and third terms are the mean and eddy flux divergence, respectively. Because of a transient nature of the CFC tracer, the time-tendency term is expected to be comparable in magnitude to all other terms in the left-hand side of (3). This makes the transient CFC balance (3) different from a steady state buoyancy balance of, for example, *Henning and Vallis* [2004], in which the time tendency term is negligible, and mean and eddy divergence terms nearly compensate each other. The right hand side is the diffusion, which is split into its lateral and vertical components. Note that, in the absence of diffusion, negative divergence of CFC fluxes acts to increase the CFC concentration. The mean diffusion terms are verified to be very small, and in regions of where CFC reaches a steady state the divergences of mean and eddy fluxes nearly balance each other. The mean fluxes are, however, much larger than the eddy fluxes in the interior of the domain.

[37] For the flux divergence terms shown in this paper, an 8-year time average was used. The transient nature of the

Table 2. CFC Drawn Down by the Eddy Resolving Experiments

	FULL_ADV	MEAN_ADV	MEAN_PLUS
Total CFC drawn into the model, mols	35.8×10^6	42.3×10^6	46.6×10^6
Upper layers: 0-250 m, roughly $\sigma_\theta < 27.6$ kg m^{-3}	18.1×10^6	18.5×10^6	18.3×10^6
Mid-depths: 250–1000 m, roughly $27.6 < \sigma_\theta < 27.8$ kg m^{-3}	12.8×10^6	13.4×10^6	17.6×10^6
Deep-depth layers: 1000–3000 m, roughly $27.8 < \sigma_\theta < 28$ kg m^{-3}	4.87×10^6	10.4×10^6	10.6×10^6

CFC can complicate the interpretation of the mean and eddy terms in (2). To examine how much of an impact different averaging periods may have, we compared the eddy flux divergence calculated using two-year fields and eight-year time averaging (not shown). The flux divergence terms differ in some locations, however, for most of the domain, the two-year and eight-year mean fields are very similar.

[38] In the remainder of this section, we use the differences between the CFC distribution in experiments FULL_ADV, MEAN_ADV and MEAN_PLUS to discuss the role of mesoscale eddies. We begin with a description of the CFC distribution differences in section 3.1. Then the subsequent sections take a detailed look at the processes that lead to the differences: interaction between eddies, surface fluxes and convection (section 3.2), interaction between eddies and sinking (section 3.3), and the interaction between eddies and mean horizontal circulation (section 3.4).

3.1. CFC Distribution With Eddy Advection is Removed

[39] There is an appreciable difference between all three runs in the total amount of CFC drawn into the ocean, the CFC burden (Table 2). For this calculation, we define the upper layers as 0–250 m (approximately σ_θ = 26.50–27.55 kg/m^3), middepths as z = 250 m–1000 m (σ_θ = 27.6–27.75 kg/m^3) and deep layers as z = 1000–3000 m (σ_θ = 27.8–28.0 kg/m^3). The run that uses the complete velocity field for advection of CFC (FULL_ADV) has a smaller CFC burden than either of the runs with the eddy advection removed. Integrated over the entire domain, FULL_ADV has 35.8×10^6 Mols, MEAN_ADV has 42.3×10^6 Mols, and MEAN_PLUS has 46.6×10^6 Mols. The differences in CFC burden are reflected in the vertical and horizontal distributions of CFC.

[40] In the uppermost layer, the surface flux forces FULL_ADV, MEAN_ADV and MEAN_PLUS to have nearly identical CFC distributions. Also, within the high latitudes, the runs all have CFC surface flux maxima at the same locations: the areas of active convection and the areas of strong surface advection (as discussed in section 2.4). However, these maxima are much stronger in the two runs without eddies, MEAN_ADV and MEAN_PLUS, compared to the FULL_ADV run. This is caused by differences in the removal of CFC from the surface, due to interaction of eddy fluxes with convection and mean advection (discussed in sections 3.2 and 3.4).

[41] In the middepths of the subpolar gyre, which correspond to isopycnals σ_θ = 27.6–27.8 in this model, FULL_ADV has about the same area-averaged CFC concentration as MEAN_ADV: 12.8×10^6 Mols versus 13.4×10^6 Mols, but the distribution differs, vertically and horizontally. In the vertical, MEAN_ADV has more CFC on the deeper isopycnals, and less on the shallow isopycnals. Figure 4b shows FULL_ADV has more CFC on σ_θ = 27.7, however, this "surplus" in FULL_ADV is averaged out by the opposite being true at 27.8. The concentration of CFC in MEAN_ADV is very high within the western boundary current and the SRF; these regions appear to be the preferred pathways for the CFC in this model (Figure 4b). In FULL_ADV, the preferred pathways are also apparent (Figure 2b), but to a lesser degree than in MEAN_ADV. Instead, the CFC is spread more uniformly throughout the middepths of the subpolar gyre. The cross-section at 40°W shown in Figure 3 also demonstrates the massive difference in the subpolar gyre interior. MEAN_ADV has very small CFC concentrations in the interior of the gyre. Instead, the CFC is concentrated within the SRF; this is seen in Figure 3b as a CFC local maximum at 50°N that extends from the surface to 3000 m.

[42] The second experiment without eddies, MEAN_PLUS, utilizes isopycnal diffusion as a substitute for eddy effects on CFC. As a result of isopycnal diffusion, the CFC spreads more uniformly, reminiscent of FULL_ADV. In the interior of the western subpolar gyre, in particular, the differences between MEAN_PLUS and FULL_ADV are smaller than those between MEAN_ADV and FULL_ADV; compare Figures 4b and 5b. In some parts of the subpolar gyre, however, the CFC distribution in MEAN_PLUS becomes even more different from FULL_ADV than it is in MEAN_ADV. For example, the eastern portion of the subpolar gyre in MEAN_PLUS has more CFC than FULL_ADV or MEAN_ADV on σ_θ = 27.7. The largest differences between MEAN_PLUS and FULL_ADV are seen within the preferred mean pathway, the SRF; see Figures 5a and 5b for σ_θ = 26.6 and 27.7. Somewhat unexpectedly, the isopycnal diffusion appears to increase CFC concentration within the SRF–the effect not exhibited by the actual eddies in FULL_ADV. We explain this effect in the following section by the increased uptake of CFC in MEAN_PLUS. Again, this is also clearly seen in the cross-section at 40°W, Figure 3d.

[43] In the deep waters of the subpolar gyre, beneath 1000 m or below the σ_θ = 27.8 isopycnal, FULL_ADV has much less CFC than both MEAN_ADV and MEAN_PLUS; see Figures 4c and 5c for σ_θ = 27.9. The maximum CFC concentrations in the FULL_ADV run are in the northwest corner of the subpolar gyre interior, and along the western boundary. Throughout the eastern interior of the deep subpolar gyre, the CFC concentration is small, but uniformly distributed. As expected, MEAN_ADV exhibits very high CFC concentrations within the SRF (Figure 4c). Also the cross-section, Figure 3b shows that the deep region of MEAN_ADV has high CFC concentrations along the northern boundary and in the SRF (near 50°N). The CFC in the deep portion of the return flow has been advected from the north boundary and not from the upper layers, because the vertical advection is very weak along the western boundary and in the return flow. In addition, there is much more

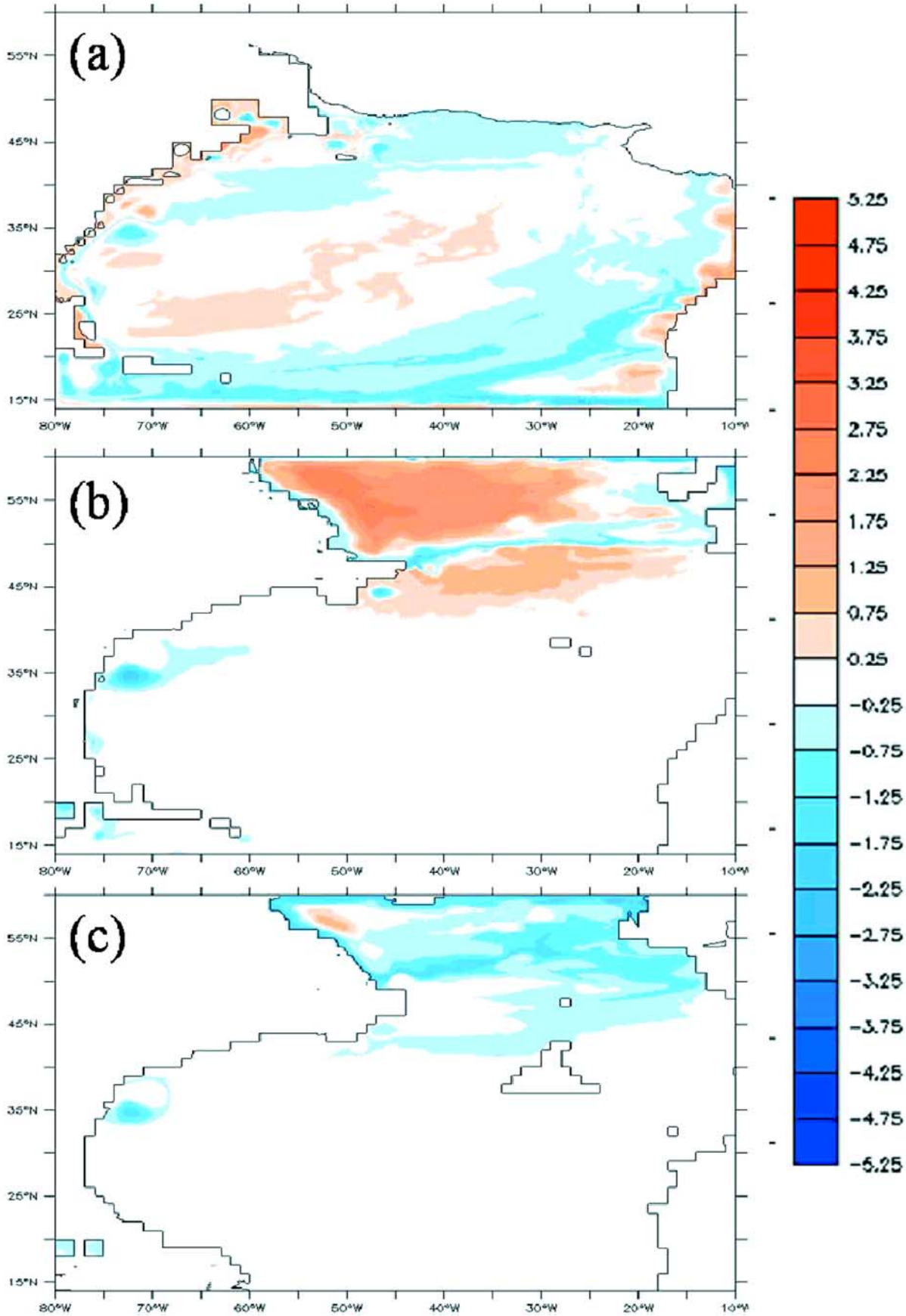

Figure 4. FULL_ADV - MEAN_ADV (FULL_ADV minus MEAN_ADV) for CFC concentration, at year 70 for: (a) σ_θ = 26.6, (b) σ_θ = 27.7 and (c) σ_θ = 27.9. Units: pmol kg^{-1}.

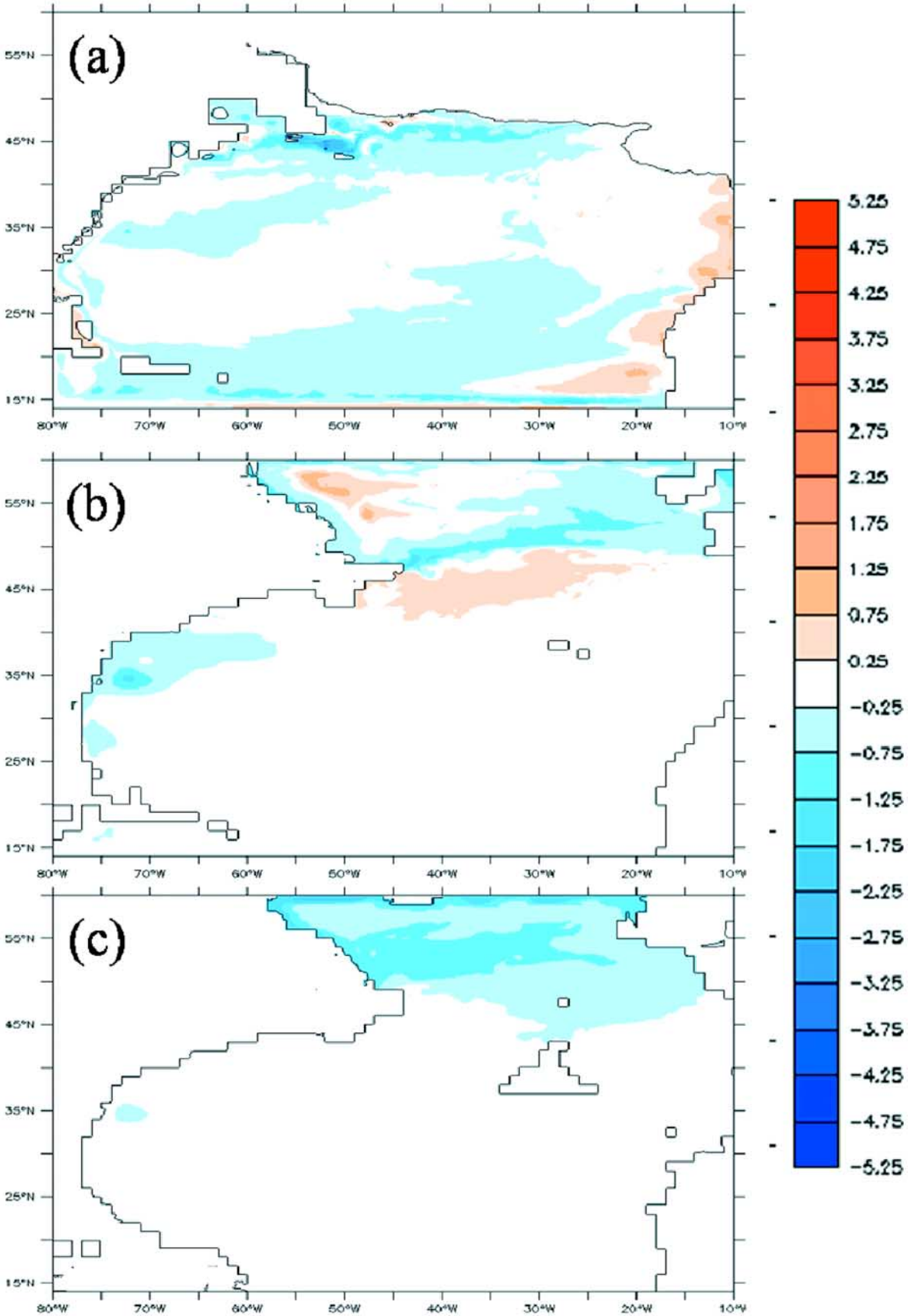

Figure 5. FULL_ADV - MEAN_PLUS for CFC concentration, at year 70: (a) $\sigma_\theta = 26.6$, (b) $\sigma_\theta = 27.7$ and (c) $\sigma_\theta = 27.9$. Units: pmol kg^{-1}.

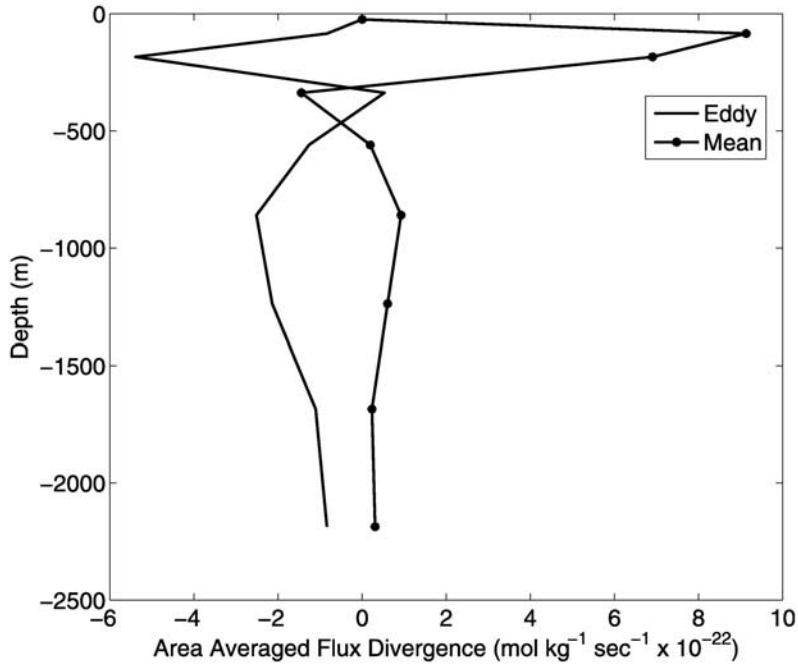

Figure 6. Area averaged flux divergence in the convective column at 58°N by 40°W. Units: (mol kg^{-1} s^{-1}) $\times 10^{-22}$.

CFC in deep layers in MEAN_ADV than in FULL_ADV throughout most of the subpolar gyre, with the exception of the north-west corner (Figure 4c). This spreading of CFC into the gyre's interior is driven by mean meridional advection, since the characteristic timescale for explicit diffusion in the model is on the order of thousand years. The spreading of CFC by the mean circulation in MEAN_ADV is further enhanced by the added isopycnal diffusion in MEAN_PLUS (Figure 5c). It is noteworthy that the NER simulation also exhibits higher CFC concentrations in the deep layers.

[44] The temperature dependence of the surface flux, and the existence of strong convection in the high latitudes cause the majority of the CFC to be in the high latitudes. However, mesoscale eddies also influence the CFC distribution in the subtropical gyre in the model. The main differences are the drawdown of CFC into the gyre's interior and the exchange between the subpolar gyre and the subtropical gyre. In the FULL_ADV run, at, $\sigma_\theta = 26.6$ there is a uniform concentration of CFC between 70° W and 55° W and 20° N and 27° N, which is missing in the MEAN_ADV run (Figure 4a). The transport of CFC from the subpolar gyre to the subtropical gyre in the eastern part of the domain is greater in the MEAN_ADV run, as can be seen in Figure 4a. This is caused by the stronger concentrations of CFC in the mean currents that flow north to south on the eastern side of the model. Figure 5a shows that the isopycnal diffusion is able to capture some of the spreading of CFC in the subtropical gyre interior, which brings CFC distribution in the subtropical gyre in MEAN_PLUS closer to that in FULL_ADV.

3.2. Interaction of Eddies and Convection and Its Effects on Surface Fluxes

[45] One of the processes that cause the surface flux maxima in the MEAN_ADV and MEAN_PLUS runs to be larger than those of FULL_ADV is the interaction between eddy advection and convection. Since the temperature fields and wind-forcing are identical for the three runs, the differences in the surface flux reflect differences in the rates of removal of CFC from the uppermost layer. For the MEAN_ADV and MEAN_PLUS runs, the surface flux in the area around 58°N and 40°W for the final 40 years of the integration is considerably larger than that of FULL_ADV, which indicates stronger uptake of CFC in the two cases without eddies. As this is a location of active convection, we investigate below the mean and eddy flux divergence in the convective column and will demonstrate that the eddy fluxes in this region are acting to damp convective removal.

[46] As can be shown by the following argument, convection acts to enhance the CFC uptake by the ocean. The atmospheric concentration of CFC increases exponentially with time, and this causes the surface layers to have more CFC than the layers beneath; setting up a vertical gradient. Since convective mixing homogenizes the tracer concentration within the column, convection then acts to remove the CFC from the surface. The surface flux responds to convective mixing by adding more CFC to the ocean. Therefore a decrease in the convective removal of CFC from the surface will weaken the CFC uptake by the ocean. Since the intensity of convection is identical in all three cases, the only factor that controls the convective flux of CFC is the distribution of CFC itself.

[47] The lateral eddy fluxes act to decrease the convective removal of CFC from the surface, as a comparison of runs with and without eddies demonstrates. This is because the eddy mixing in FULL_ADV increases the concentration of CFC in the bottom layers of the convection column, which decreases the vertical CFC gradient in the column and weakens the convective flux of the tracer. To illustrate this point, Figure 6 shows the mean and eddy flux divergence averaged over the area of the convective column at 40°W

58°N. The eddy flux divergence is 'filling' this convective water column with CFC, while the mean flux divergence is 'evacuating' CFC from the region. Removing the eddies in the MEAN_ADV run makes the region an area of advective removal of CFC, which in turn causes the convective mixing to draw more CFC out of the surface layer. This causes the surface flux to respond by increasing, leading to a larger CFC uptake. This mechanism contributes to very high CFC concentration in the deep layers in MEAN_ADV.

[48] The isopycnal diffusion in MEAN_PLUS is working in the direction *opposite* of that of eddies in FULL_ADV. The surface flux/convection interaction brings more CFC into the bottom of the convection region as compared to the areas around it, setting up a lateral gradient. In the MEAN_PLUS run, the down-gradient diffusion responds by fluxing CFC away from the deeper portions of the convective column. The result is a CFC uptake that is larger than even the case without eddies and diffusion, MEAN_ADV. Thus because of the "filling" effect of eddy advection in and around the convective column, and "evacuating" effect of diffusion, FULL_ADV has the smallest CFC uptake and MEAN_PLUS has the largest. This also explains why isopycnal diffusion appears to increase CFC concentration within deep SRF (Figure 5c).

[49] It is noteworthy, that in the northeast corner of the model, the opposite occurs. The eddy advection near the bottom of the convective column there acts to remove CFC from the convection region. As a result, the surface flux in MEAN_PLUS and FULL_ADV is nearly equal in the region of this convective column, but it is smaller in the MEAN_ADV case. However, the convective column in the northeast corner is shorter and does not sit along the preferred path of the CFC in the mean currents. Therefore its impact on the CFC burden is not as significant as the large convective column near 58°N by 40°W.

[50] For both of these convective columns, we also calculated the mean and eddy flux divergence of density (not shown). The eddy flux divergence of density acts to make the upper layers of the convective columns lighter at a faster rate than the bottom layers. Thus the eddies are aiding in the restratification. This is in qualitative agreement with the previous studies on eddies in convective columns [*Legg et al.*, 1998; *Jones and Marshall*, 1997; *Marshall et al.*, 2002], which investigate the role of baroclinic instability in the presence of convection. This dissipation of the positive density anomaly in the bottom of the convective columns is in contrast to the "filling" effect of eddies on CFC in the convective column near 40°W. The direction of the eddy flux of a tracer relative to the mean tracer gradient is, however, determined by several processes. *Wilson and Williams* [2006] demonstrate that up-gradient eddy fluxes are possible if there is a source of tracer variance. Since convection delivers CFC anomalies to the bottom layers, it will act to increase the variance and, therefore, induce upgradient fluxes of CFC. This action of convection is counterbalanced by dissipation; advection of variance also plays a big role. The resulting balance is apparently different for density and CFC. Our model is, however, unlikely to resolve all spatial scales important for eddy interaction with the convective column. The detailed investigation of the balance for the CFC/density variance in convective regions can become a subject of a future study with a model of higher spatial resolution.

3.3. Eddies, Sinking, and the CFC Distribution in the Deep Waters

[51] A comparison of the CFC concentration in the deeper levels of the three runs shows that the eddies effectively control the amount of CFC that reaches the deep layers. The amount of CFC at depth is much greater in MEAN_ADV compared to FULL_ADV (Figure 4c); see also the cross sections at 40°W (Figure 3). In total, less than 14% of the CFC penetrates deeper than 1000 m in the FULL_ADV run, while more that 24.5% does so in MEAN_ADV (Table 2). Also, almost five times more CFC is transported below 1500 m in the MEAN_ADV run.

[52] The largest downward velocities are along the northern boundary. These are the locations where active sinking (downwelling) of waters takes place. In a simplified, two-layer picture of the thermohaline circulation [*Schmitz*, 1996], the sinking links the northward flowing thermocline waters with the southward flowing NADW, thus closing the Atlantic MOC cell. Sinking takes place over narrow regions and reaches deep layers in our model. In contrast, convection is not associated with the net mass flux [*Send and Marshall*, 1995; *Klinger et al.*, 1996], and the deepest convective column in the model spans from the surface to 400 m. On a horizontal plane, locations of convection and sinking do not coincide; see *Marotzke and Scott* [1999] for a detailed discussion. The mean currents advect the CFC toward the sinking regions along the northern boundary. Near the sinking regions the divergence of eddy fluxes (not shown) acts to remove CFC from the sinking region, decreasing the downward flux of CFC. In the absence of eddies, the CFC accumulates at these locations allowing more of it to be transported downward.

[53] In MEAN_PLUS, the diffusion also acts to spread some of the CFC away from the sinking regions. However, the eddy flux divergence in FULL_ADV near the sinking regions appears to be much stronger than the isopycnal diffusion in MEAN_PLUS, causing the FULL_ADV to have less CFC in the deep layers (Table 2). To examine this further, the CFC burden in the deep water in MEAN_PLUS is compared for the simulation similar to MEAN_PLUS which used an isopycnal diffusion constant of 1000 $m^2\ s^{-1}$ (as compared to MEAN_PLUS which used 100 $m^2\ s^{-1}$). In the run with stronger diffusion, the CFC concentration in the sinking regions and in the deep water is less than in MEAN_PLUS, and is very similar to that in FULL_ADV, confirming the strong diffusion-like effect of the eddies near the sinking region. Large explicit diffusion in this run, however, leads to drastic differences with the FULL_ADV elsewhere in the upper and middepth of the model; the results of the run with diffusion coefficient of 1000 $m^2\ s^{-1}$ are not shown here.

3.4. Eddy Flux Divergence and the Subpolar Gyre Interior

[54] In the middepth of the subpolar gyre, (Figure 4b) FULL_ADV has much more CFC than MEAN_ADV suggesting that the eddies are spreading CFC into the subpolar gyre interior away from SRF. To examine this conjecture quantitatively, we compare the mean and eddy

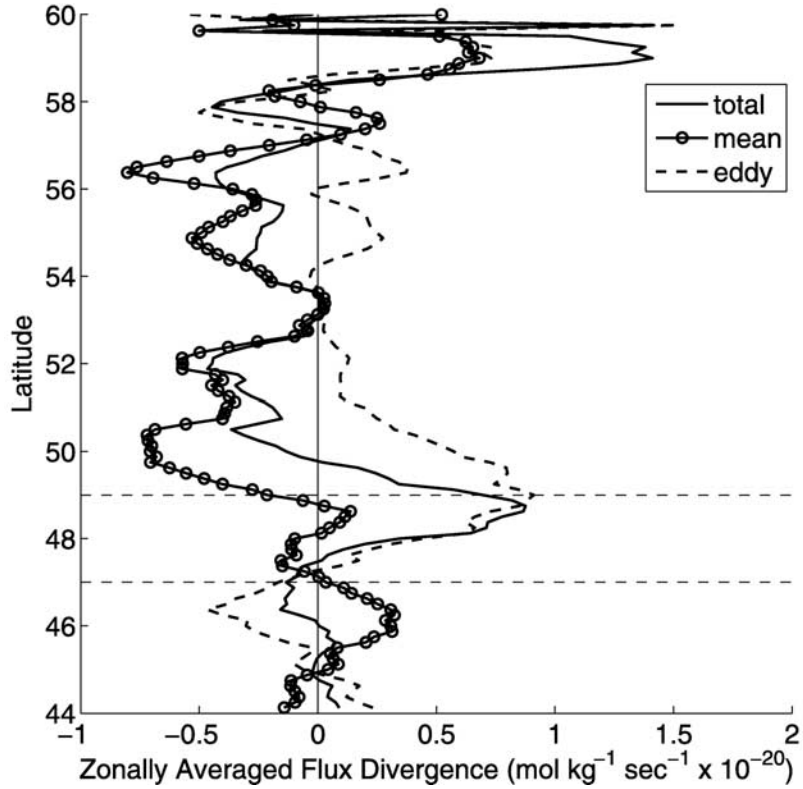

Figure 7. CFC flux divergence, zonally averaged between 45°W and 35°W in the subpolar gyre. The dashed horizontal lines serve to demarcate the location of the SRF. Units: mol kg^{-1}s^{-1}.

flux divergence for the subpolar gyre. Figure 7 shows the zonal average of the total CFC flux divergence for a region from 45° W to 35° W in the subpolar gyre on isopycnal 27.7. For this region, the strongest concentration of CFC in MEAN_ADV is located between 47°N and 50°N; this the location of SRF in the model. Within SRF, at approximately 48°N, the eddies in the FULL_ADV run act to remove (positive divergence, as shown in the figure) CFC from this region; the total divergence is dominated by the eddy term. North of 50°, all the way to 57°N, eddies continue to remove CFC from the region, although the eddy flux divergence is rather small, especially south of 54°N. In contrast, the mean advection acts to fill the gyre interior with CFC and clearly dominates the total flux divergence.

[55] The above analysis demonstrates that the mean currents are responsible for filling the gyre interior, which may seem in contradiction to the lack of CFC in the gyre interior in MEAN_ADV, which uses the same mean velocity as FULL_ADV. However, it is important to understand that MEAN_ADV is lacking a mechanism of removal of CFC from the preferred mean path of SRF; this removal is achieved by eddies in FULL_ADV. The spreading of CFC into the gyre interior is, therefore, a result of the joint work by both eddy and mean advection. The effect of eddies on CFC distribution in the subpolar gyre interior is fundamentally non-local.

[56] As demonstrated above, the eddy flux divergence removes CFC from the mean currents of the SRF, thus acting similarly to the downgradient diffusion. Since MEAN_PLUS uses explicit down-gradient diffusion in place of eddies, there is a justifiable expectation that MEAN_PLUS and FULL_ADV would have similar CFC distributions in this region. The MEAN_PLUS with the diffusivity of 100 m^2 s^{-1} has more CFC than FULL_ADV along the SRF and just to the north of it, and less CFC south of the SRF (Figure 5b). These differences suggest that this run does not have enough eddy-driven spreading of CFC away from SRF, and the isopycnal diffusion is simply not strong enough. Confirming this conclusion, increasing diffusivity to 1000 m^2 s^{-1} in MEAN_PLUS helps to decrease the difference with FULL_ADV in the vicinity of SRF. The run with a large diffusivity, however, exhibits very large CFC biases elsewhere in the domain (see also section 3.3). Northward from SRF, where the eddy flux divergence is small and CFC spreading is governed by the mean advection, MEAN_PLUS and FULL_ADV have nearly equal CFC distributions.

[57] This comparison of eddy fluxes (resolved or replaced with diffusion) of CFC at middepths in the FULL_ADV and MEAN_PLUS model runs has another complication. The impacts of the eddy fluxes on convection, discussed in section 3.2, cause the amount of CFC in the SRF and being delivered to the sinking regions to be greater in MEAN_PLUS than FULL_ADV. This impact is clearly shown in Figure 5b, in the northeast corner of the subpolar gyre (52°W by 55°N), where FULL_ADV has more CFC.

4. Summary and Discussion

[58] This study examines the role of mesoscale eddies in distribution of a transient, passive tracer, CFC, in a numer-

ical model of the North Atlantic. Such distribution is determined by a number of processes, whose effects on CFC are interwoven in a complex way. This study uses the most straightforward and transparent method of isolating the role of eddies in such a complex dynamical system. Our main conclusions are based on the comparison of two experiments, one with and one without eddy advection of CFC, FULL_ADV and MEAN_ADV, respectively. The experimental set-up utilized an offline advection method in which both the time-mean circulation and density structure were identical in the two experiments. The differences between FULL_ADV and MEAN_ADV were, therefore, caused by the presence of eddy advection in the former run. The CFC distributions in these two experiments exhibit two main differences.

[59] (1) In the upper 1000 m, FULL_ADV has CFC throughout the subpolar gyre interior, while in MEAN_ADV CFC is strongly concentrated within a boundary current (SRF) that enclosed the subpolar gyre.

[60] (2) Below 1500 m, FULL_ADV has very little CFC, while MEAN_ADV has significant amounts of CFC concentrated within SRF.

[61] To aid in understanding the differences, and also test the assumption that eddies can be replaced with constant down-gradient diffusion, we also ran the experiment MEAN_PLUS. The analysis of all three runs showed that: (1) interactions of eddy advection with convection and mean advection in several locations can have a substantial impact on basin-wide tracer distribution; and (2) the corresponding eddy fluxes cannot be successfully represented by downgradient diffusion with a constant coefficient, even if the mean velocity field and density structure include the proper effects of eddies.

[62] The horizontal spreading of CFCs from the subpolar gyre return flow (SRF) throughout the subpolar gyre is driven by combined effects of the eddy and mean advection. Local eddy fluxes in the gyre interior, however, do not play a major role in the process, and northward of SRF, the eddy flux divergence is weak. Instead, the main affect of eddies is to disperse CFC away from SRF; then the mean advection spreads the CFC throughout the gyre interior. Eddy flux divergence is large within and southward of SRF suggesting substantial mixing of CFC into the North Atlantic Current. Using a too small diffusivity in MEAN_PLUS consequently leads to too much CFC north of and too little CFC south of SRF. Prescribing larger diffusivity, however, leads to very strong biases in other regions of the model.

[63] Eddy activity in a few locations can have dramatic effects on the surface uptake and deep concentrations of CFC. This is especially true within and near convective columns, and near sinking sites. By filling the deep part of the convective column at 40°W with CFC, the eddies inhibit convective removal of CFC from the surface and thus weaken the surface intake from the atmosphere. In contrast, eddies act to flux CFC downgradient and away from the sinking sites. Both of these effects lead to lower total CFC burden in FULL_ADV compare to the two runs without eddies, MEAN_ADV and MEAN_PLUS. Eddies thus effectively act to limit the amount of CFC drawn into the ocean; the uptake of CFC in non-eddy resolving models with diffusion is likely to be overestimated.

[64] In addition, CFC distribution is often a result of several processes, some of them taking place in distant parts of the domain. In particular, spreading of CFC by the mean currents in the subpolar gyre interior is controlled by the removal of CFC from SRF by eddies, and by concentration of CFC within SRF itself. As the amount of CFC within SRF is controlled by the CFC uptake within the convection sites, and eddies act to inhibit such uptake, general increase in the eddy activity will decrease the supply of CFC into midlatitudes, but will increase CFC removal from SRF.

[65] These results emphasize difficulty in modeling complex, often non-local effects of eddies by downgradient diffusion with a constant coefficient. Errors in representing eddy fluxes in several locations, such as convective and sinking sites and SRF, lead to wide-spread biases in CFC concentration, and a model with a constant diffusivity is certainly a bad choice. This is further illustrated by the MEAN_PLUS experiment, in which isopycnal diffusion is added to MEAN_ADV experiment in lieu of explicit eddies. The resulting CFC distribution is qualitatively different from FULL_ADV, emphasizing, in particular, the non-diffusive nature of eddy transports in some locations, most notably near the convection sites. Eddy fluxes in other locations can, in principle, be approximated by diffusion with geographically varying coefficients: such as in regions north of SRF (near-zero diffusivity), and south of SRF (strong diffusivity). Identifying dependence of the diffusivity on large scale fields, i.e., suggesting an appropriate closure, seems challenging and is beyond the scope of this paper.

[66] The traditional approach of comparing the FULL_ADV and a non-eddy resolving version of the model shows the drastic influence of changing resolution. However, with respect to the role of eddies the results are unclear, because of drastic differences in the mean circulation. These differences are partly due to different horizontal resolution and, therefore, width and intensity of the boundary currents. Another reason is in the effects of eddies on stratification. In an extension of the MEAN_ADV experiment, another offline experiment is conducted in which the time mean velocity field advect all of the tracers, including temperature and salinity. In this experiment, temperature and salinity are treated as passive tracers, and so their distribution does not affect the velocities. This experiment, therefore, cannot be used to identify the full role of eddies in setting the stratification in the ocean. However, it can give a suggestion as to whether the eddies are important for maintaining the steady state stratification. Using only the mean velocity causes a significant change in the temperature and salinity distribution. In the subtropical gyre, the thermocline deepens. This supports the results of *Henning and Vallis* [2004] that show that eddy fluxes help to maintain the thermocline.

[67] This study analyzes effects of eddies in the most direct and transparent way: by contrasting simulations with and without eddies. Other methods, involving comparison of eddy-resolving and non-eddy-resolving simulations or analysis of the balances in the main equations generally lead to less easy-to-interpret results. We note, however, that the isolation of the direct eddy effects is only possible when one considers distribution of a dynamically passive tracer, whose distribution does not influence the circulation. Even

in such a case (our experiment MEAN_ADV) the indirect effects of eddies on CFC are still present via distribution of the mean circulation, surface temperature and of the convection.

[68] In our study, the transient nature of CFCs allows a closer look at the ways that atmospheric gases are moved from the surface into the deeper regions of the model's subpolar gyre, mainly through convection and advection by mean currents and eddies. These real-ocean pathways may not be simulated by our intermediate complexity model in full detail, due to a number of idealizations, and there are some noticeable biases in the simulated distribution of CFC. This study, nevertheless, demonstrates an important role of eddies in all main processes that distribute atmospheric gases in the real ocean: uptake by the ocean surface, convection, and advection.

[69] Modeling the ocean pathways of chemicals drawn down from the atmosphere has become increasingly important in recent years [*Sabine et al.*, 2004]. However, the models continue to show deficiencies, leading to substantial efforts in tracking down possible causes to the model biases. While SGS parameterizations are often mentioned as possible contributors to the errors, their quantitative impacts and the locations of their importance are largely unknown [e.g., *Doney et al.*, 2004]. Here we show that the locations of convection, sinking and strong isopycnal advection are the key areas to focus attention when attempting to parameterize eddies.

[70] Previous ER modeling work has shown that resolving mesoscale eddies leads to differences with non-eddy-resolving models that use SGS parameterizations. This paper agrees with those findings, and it also shows conclusively that the differences are large and merit attention, especially for chemical tracer modeling. This research also suggests that attention must be paid to the interactions between the mesoscale eddies and convection in future models that utilize higher resolution; see also *Visbeck et al.* [1996]. We conclude by emphasizing that an offline model with eddy advection removed represents a powerful tool for the analysis of the role of eddies on the distribution of a dynamically passive tracer and testing parameterization schemes.

[71] **Acknowledgments.** We thank Pavel Berloff, LuAnne Thompson and E.S. Sarachik for helpful advice on experimental strategy and interpretation of results, and Rolv Sonnerup and John Bullister for guidance in including CFC in our model. We are thankful for suggestions on improving the text by two anonymous reviewers. This work was supported by the National Science Foundation under grant 0346178.

References

Beismann, J. O., and R. Redler (2003), Model simulations of CFC uptake in North Atlantic deep water: Effects of parameterizations and grid resolution, *J. Geophys. Res.*, *108*(C5), 3159, doi:10.1029/2001JC001253.

Bey, I., D. J. Jacob, R. M. Yantosca, J. A. Logan, B. Field, A. M. Fiore, Q. Li, H. Liu, L. J. Mickley, and M. Schultz (2001), Global modeling of tropospheric chemistry with assimilated meteorology: Model description and evaluation, *J. Geophys. Res.*, *106*(D19), 23,073–23,095.

Boyer, T., S. Levitus, H. Garcia, R. Locarnini, C. Stephens, and J. Antonov (2005), Objective analyses of annual, seasonal, and monthly temperature and salinity for the World Ocean on a 0.25 degree grid, *Int. J. Climatol.*, *25*, 931–945.

Bryan, F. (1987), Parameter sensitivity of primitive equation ocean general circulation models, *J. Phys. Oceanogr.*, *17*, 970–985.

Cessi, P., and M. Fantini (2004), The eddy-driven thermocline, *J. Phys. Oceanogr.*, *34*, 2642–2658.

Doney, S. C., et al. (2004), Evaluating global ocean carbon models: The importance of realistic physics, *Global Biogeochem. Cycles*, *18*, GB3017, doi:10.1029/2003GB002150.

Dutay, J.-C., et al. (2001), Evaluation of ocean model ventilation with CFC-11: Comparison of 13 global ocean models, *Ocean Modell.*, *4*(2), 89–120.

England, M. H., and E. Maier-Reimer (2001), Using chemical tracers to assess ocean models, *Rev. Geophys.*, *39*, 29–70.

England, M. H., V. C. Garcon, and J.-F. Minster (1994), Chlorofluorocarbons uptake in a world ocean model, 1. Sensitivity to the surface gas forcing, *J. Geophys. Res.*, *99*(C12), 25,215–25,233.

Gent, P. R., and J. C. McWilliams (1990), Isopycnal mixing in ocean circulation models, *J. Phys. Oceanogr.*, *20*, 150–155.

Gille, S., and R. Davis (1999), The influence of mesoscale eddies on coarsely resolved density: An examination of subgrid-scale parameterization, *J. Phys. Oceanogr.*, *29*, 1109–1123.

Gnanadesikan, A. (1999), A simple predictive model for the structure of the oceanic pycnocline, *Science*, *283*, 2077–2079.

Gupta, A. S., and M. H. England (2004), Evaluation of interior circulation in a high-resolution global ocean model. Part 1: Deep and bottom waters, *J. Phys. Oceanogr.*, *34*, 2592–2614.

Henning, C. C., and G. K. Vallis (2004), The effects of mesoscale eddies on the main subtropical thermocline, *J. Phys. Oceanogr.*, *34*, 2428–2443.

Jones, H., and J. Marshall (1997), Restratification after deep convection, *J. Phys. Oceanogr.*, *27*, 2276–2287.

Karsten, R., H. Jones, and J. Marshall (2002), The role of eddy transfer in setting the stratification and transport of a circumpolar current, *J. Phys. Oceanogr.*, *32*, 39–54.

Key, R. M., A. Kozyr, C. L. Sabine, K. Lee, R. Wanninkhof, J. Bullister, R. A. Feely, F. Millero, C. Mordy, and T.-H. Peng (2004), A global ocean carbon climatology: Results from GLODAP, *Global Biogeochem. Cycles*, *18*, GB4031, doi:10.1029/2004GB002247.

Klinger, B. A., J. Marshall, and U. Send (1996), Representation and parameterization of deep convective plumes by mixing, *J. Geophys. Res.*, *101*(C8), 18,175–18,182.

Ladd, C., and L. Thompson (1998), The influence of eddies on tracer transport in the abyssal ocean, *J. Phys. Oceanogr.*, *28*, 1717–1738.

Ledwell, J. R., A. J. Watson, and C. S. Law (1993), Evidence for slow mixing across the pycnocline from an open-ocean tracer-release experiment, *Nature*, *364*, 701–703.

Legg, S., J. M. McWilliams, and J. Gao (1998), Localization of deep convection by a mesoscale eddy, *J. Phys. Oceanogr.*, *28*, 944–970.

Marotzke, J., and J. R. Scott (1999), Convective mixing and the thermohaline circulation, *J. Phys. Oceanogr.*, *29*, 2962–2970.

Marshall, J., and T. Radko (2003), Residual-mean solutions for the Antarctic Circumpolar Current and its associated overturning circulation, *J. Phys. Oceanogr.*, *33*, 2341–2354.

Marshall, J., H. Jones, R. Karsten, and R. Wardle (2002), Can eddies set ocean stratification?, *J. Phys. Oceanogr.*, *32*, 26–38.

McWilliams, J. C. (2008), The nature and consequences of oceanic eddies, in *Eddy-Resolving Ocean Modeling*, edited by M. Hecht and H. Hasumi, *AGU Monograph*, in press.

Nakamura, M., and Y. Chao (2000), On the eddy isopycnal thickness diffusivity of the Gent-McWilliams subgrid mixing parameterization, *J. Clim.*, *13*, 502–510.

Pacanowski, R. C., and S. M. Griffies (1999), MOM 3 manual, Technical Report, GFDL/NOAA, Princeton, NJ.

Pickart, R. S., and M. A. Spall (2007), Impact of Labrador Sea convection on the North Atlantic meridional overturning circulation, *J. Phys. Oceanogr.*, *37*, 2207–2226.

Radko, T., and J. Marshall (2004), Eddy-induced diapycnal fluxes and their role in the maintenance of the thermocline, *J. Phys. Oceanogr.*, *34*, 372–383.

Roberts, M., and D. Marshall (2000), On the validity of downgradient eddy closures in ocean models, *J. Geophys. Res.*, *105*(C12), 28,613–28,627.

Sabine, C. L., et al. (2004), The ocean sink for anthropogenic CO_2, *Science*, *305*(5682), 367–371.

Schmitz, W., Jr. (1996), On the world ocean circulation, vol. 1, Some global features/North Atlantic circulation, Technical Report WHOI-96-03, Woods Hole Oceanographic Institution, Woods Hole, Mass.

Send, U., and J. Marshall (1995), Integral effects of deep convection, *J. Phys. Oceanogr.*, *25*, 855–872.

Smith, R. D., M. Maltrud, F. O. Bryan, and W. Hecht (2000), Numerical simulation of the North Atlantic Ocean at $^1/_{10}°$, *J. Phys. Oceanogr.*, *30*, 1532–1561.

Solovev, M. A. (1999), Assessment of mesoscale eddy parameterizations for coarse resolution ocean models, Ph.D. thesis, WHOI/MIT, Cambridge, Mass.

Toole, J. M., K. L. Polzin, and R. W. Schmitt (1994), Estimates of diapycnal mixing in the abyssal ocean, *Science*, *264*, 1120–1123.

Visbeck, M., J. Marshall, and H. Jones (1996), Dynamics of isolated convective regions in the ocean, *J. Phys. Oceanogr.*, *26*, 1721–1734.
Wanninkhof, R. (1992), Relationship between wind speed and gas exchange over the ocean, *J. Geophys. Res.*, *97*(C5), 7373–7382.
Warner, M. J., and R. F. Weiss (1985), Solubilities of chlorofluorocarbons 11 and 12 in water and seawater, *Deep Sea Res.*, *32*, 1485–1497.
Wilson, C., and R. G. Williams (2006), When are eddy fluxes directed downgradient?, *J. Phys. Oceanogr.*, *36*, 189–201.

J. Booth, Department of Atmospheric Sciences, University of Washington, Box 351640, Seattle, WA 98195, USA.
I. Kamenkovich, Rosenstiel School of Marine and Atmospheric Science, Division of Meteorology and Physical Oceanography, 4600 Rickenbacker Causeway, Miami, FL 33149, USA. (ikamenkovich@rsmas.miami.edu)